Received: 3 May 2022 | Revised: 18 July 2022 | Accepted: 2 August 2022

DOI: 10.1002/jex2.57

RESEARCH ARTICLE

Active antithrombin glycoforms are selectively physiosorbed on plasma extracellular vesicles

Annalisa Radeghieri[1,2] | **Silvia Alacqua**[1] | **Andrea Zendrini**[1,2] | **Vanessa Previcini**[1] | **Francesca Todaro**[1] | **Giuliana Martini**[3] | **Doris Ricotta**[1,4] | **Paolo Bergese**[1,2,5]

[1]Department of Molecular and Translational Medicine, University of Brescia, Brescia, Italy

[2]Center for Colloid and Surface Science (CSGI), Florence, Italy

[3]Clinical Chemistry Laboratory, Spedali Civili Hospital, Brescia, Italy

[4]GLG Klinikum Barnim GmbH, Werner Forßmann Klinikum Eberswalde, Eberswalde, Germany

[5]Institute for Research and Biomedical Innovation (IRIB), National Research Council, Palermo, Italy

Correspondence
Annalisa Radeghieri, Department of molecular and Translational Medicine, University of Brescia, Viale Europa 11, 25123 Brescia, Italy.
Email: annalisa.radeghieri@unibs.it

Funding information
Ministero dell'Istruzione, dell'Universitlà e della Ricerca, Grant/Award Number: Grant No. 2017E3A2NR_004

Abstract

Antithrombin (AT) is a glycoprotein produced by the liver and a principal antagonist of active clotting proteases. A deficit in AT function leads to AT qualitative deficiency, challenging to diagnose. Here we report that active AT may travel physiosorbed on the surface of plasma extracellular vesicles (EVs), contributing to form the "EV-protein corona." The corona is enriched in specific AT glycoforms, thus suggesting glycosylation to play a key role in AT partitioning between EVs and plasma. Differences in AT glycoform composition of the corona of EVs separated from plasma of healthy and AT qualitative deficiency-affected subjects were also noticed. This suggests deconstructing the plasma into its nanostructured components, as EVs, could suggest novel directions to unravel pathophysiological mechanisms.

KEYWORDS
antithrombin, extracellular vesicles, glycosylation, protein corona

1 | INTRODUCTION

Antithrombin (AT), a heparin cofactor and member of the serine protease inhibitor (serpin) gene family, is an important protease inhibitor that regulates the function of several serine proteases in the coagulation cascade (SC B. Antithrombin III & heparin cofactor II 2001). AT physiologically inactivates thrombin (factor IIa) and factor Xa (FXa) and, to a lesser extent, factors IXa, XIa, XIIa, tissue plasminogen activator (tPA), urokinase, trypsin, plasmin, and kallikrein (Danielsson & Bjork, 1982; Persson et al., 2001). The plasma concentration of AT is 112–150 mg/L, with a half-life of 2–3 days (Mammen, 1998; Murano et al., 1980). The liver is the primary source of AT synthesis and post-translational glycosylation (Petersen & Sottrup-Jensen, 1979). Mature AT has a molecular weight of 58 kDa and four potential N-glycosylation sites at asparagine (Asn) residues, occupied by a biantennary or triantennary structure of complex N-glycans bearing two terminal sialic acids. No other post-translational modifications (PTM) are known to be present on the protein. Many isoforms of AT are documented, because of a microheterogeneity of attached carbohydrates. The 93%–94% predominant group of isoforms is designated as α-AT, while the 6%–7% subsidiary group form as β-AT: they can be isolated thanks to different binding to glycosamminoglycans (Demelbauer et al., 2004, 2005). Even if less abundant, β-AT has higher affinity for heparin and is more important in controlling thrombogenic events from tissue injury (Donges et al., 2001; Franzen et al., 1980; Kremser et al., 2003; Picard et al., 1995). Clotting inactivation by AT is the consequence of the entrapment of the coagulation factors in a covalent and equimolar complex in which the active site of the proteases becomes inaccessible to its substrate (Olson & Bjork, 1994).

AT circulates in a form that has a low inhibitory activity. Under normal physiological circumstances, the anticoagulant effect of AT is accelerated at least a thousand times in the presence of heparin-like glycosaminoglycans, such as heparan sulphates, located on the vascular endothelium. Besides, the interaction of AT with the endothelium gives rise to an anti-inflammatory effect: it increases the production of the anti-inflammatory cytokine prostacyclin, which then mediates smooth muscle relaxation and vasodilatation and inhibits platelet aggregation (Patnaik & Moll, 2008).

The evidence for the role AT plays in regulating blood coagulation is demonstrated by the correlation between inherited or acquired AT deficiencies and an increased risk of developing thrombotic disease. Inherited AT deficiency is divided into type I deficiency (T1), in which both the functional activity and levels of AT are proportionately reduced (quantitative deficiency), and type II deficiency (T2), in which normal antigen levels are found in association with low AT activity due to a dysfunctional protein (qualitative deficiency) (Lane et al., 1997).

In the last years, together with many other proteins usually considered "soluble" factors (Buzas et al., 2018), AT has also been found associated with platelet-derived extracellular vesicles (EVs) (Levin & Sukhareva, 2015) extracted from plasma or serum, and cell culture media extracted EVs (Atay et al., 2011; Luengo-Gil et al., 2019). EVs are nanoparticles released by eukaryotic cells in the form of a lipid membrane that encloses proteins, nucleic acids, and metabolites. They are today considered the third way of cell communication—other than direct intercellular physical stimuli and paracrine secretion of active molecules (Mathieu et al., 2019)—placing EV research as a key field within immunology, haematology, and cancer cell biology (Berardocco et al., 2017; Morad-Rémy et al., 2016).

The involvement of circulating EVs in coagulation processes has been documented, but their role is still debated, since both coagulation factors and anticoagulant proteins have been found associated to blood EVs (Dahlbaeck et al., 1992; Nomura, 2017; Nomura et al., 2008; Pérez-Casal et al., 2005; Tripisciano et al., 2017). This study proposes the first detailed analysis of the association of AT isoforms to circulating plasma EVs, evidencing a key role of glycosylation and disclosing a new possible perspective in understanding AT-related deficiencies.

2 | MATERIALS AND METHODS

2.1 | Patients and blood sample collection

Ethical approval was obtained from the Ethical committee of Spedali Civili hospital (Brescia, Nr.NP4761). Patients and control subjects enrolled in the study provided written consent according to the Declaration of Helsinki. Tests were performed on plasma samples obtained from the Haemophilia Centre, Haemostasis and Thrombosis Unit at Spedali Civili hospital (Brescia). Peripheral blood samples were collected from three fasting patients diagnosed with T2 AT deficiency, and five fasting healthy subjects. As described in our previous work (Grossi et al., 2020) blood samples processing was performed within 2 h from the withdrawal and samples were kept at room temperature (RT). Careful tube transportation was ensured to avoid unnecessary agitation. For this purpose, a box maintaining blood tubes in a steady vertical position was used. EDTA was added and samples were immediately centrifuged at 4200 *g* for 10 min at 22°C, with Rotixa 500RS (Hettich centrifuges, Germany), rotor nr. 4248 following Spedali Civili protocols to obtain platelets and cell-free plasma for further analyses. To this regard after centrifugation plasma was collected in a fresh plastic tube, leaving 1 cm of plasma above the buffy layer so as not to disturb it (Rikkert et al., 2021). Platelet counting was also performed with Sysmex SN10 to verify any platelet contamination (measurements available upon request). Samples were anonymized and stored at -80°C until analysis. At the time of analyses, about 1 ml of plasma was thawed at RT and examined.

2.2 | EV separation protocols

2.2.1 | Ultracentrifugation (UC) and sucrose gradient

Plasma EVs were isolated through UC and discontinuous sucrose gradient (Grossi et al., 2020). Briefly, 1 ml of plasma was processed with three subsequent steps of centrifugation at 4°C: 800 *g*, 16,000 *g* and 100,000 *g*, respectively for 30 min, 45 min, and 2 h. The supernatant was discarded, and the EV pellet was resuspended in 1 ml of buffer (250 mM sucrose 10 mM Tris-HCl, pH 7.4) and loaded at the top of a discontinuous sucrose gradient. The gradient was centrifuged at 230,000 *g* for 16 h at 4°C (rotor MLS-50, Beckman Optima MAX). Twelve fractions of 400 μl were collected from the top of the gradient and pelleted by UC at 100,000 *g* for 2 h at 4°C (Figure 1). Fractions were analyzed with SDS-PAGE and Western Blot (WB).

Subsequentially, the EV content of each sample was evaluated by the quantification of the total protein concentration through the Bradford assay.

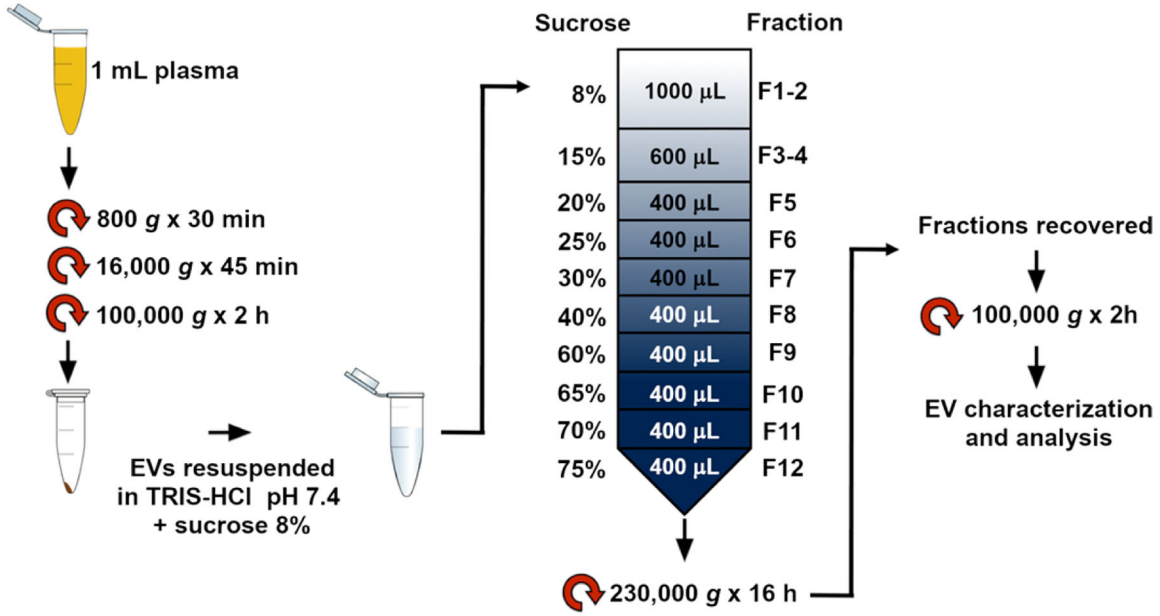

FIGURE 1 EV purification protocol. Key concept sketched. EVs were isolated from 1 ml of human plasma by differential centrifugation. The pellet was resuspended in Tris-HCl sucrose 8% and loaded on the top of a discontinuous sucrose gradient. Afterwards, 12 fractions were collected, pelleted by ultra-centrifugation, and further analyzed

2.2.2 | Size exclusion chromatography (SEC)

Plasma EVs were also isolated through SEC, using IZON qEVsingle columns (IZON Science Ltd). We performed the separation following the producer datasheet on the EVs obtained by the UC steps. EV pellet obtained from the aforementioned centrifugation steps was resuspended in 100 μl of PBS and loaded on the top of SEC columns. Fractions of 200 μl were collected and EV-enriched fractions (as indicated in the producer datasheet) 6–11 were centrifuged at 100,000 *g* for 2 h at 4°C. Pellets were resuspended and analyzed by SDS-PAGE and WB.

2.3 | EV characterization

2.3.1 | Atomic force microscopy (AFM)

EV pellets were resuspended in 50 μl of PBS and diluted 1:10 v/v with deionized water. 5–10 μl of samples were then spotted onto freshly cleaved mica sheets (PELCO® Mica discs Grade V-1, thickness 0.15 mm, 10 mm diameter from Ted Pella, Inc). All mica substrates were dried at RT and analyzed using a Nanosurf NaioAFM equipped with Multi75AI-G probes (Budget sensors). Images were acquired in dynamic mode, scan size ranged from 1.5 to 15 μm and scan speed ranged from 0.8 to 1.5 s/line. AFM images were processed using Gwyddion ver. 2.58. The size of particles was extrapolated using built-in modules. Particle size distribution was then calculated on GraphPad PRISM ver. 6, by plotting particle size against relative abundance.

2.3.2 | CONAN assay

The EV formulation was checked for purity from protein contaminants using the COlorimetric NANoplasmonic (CONAN) assay, a recognized method to determine the purity of EV preparations (Thery et al., 2018) that is based on the clustering of gold NPs onto lipid membranes (Montis et al., 2020). The CONAN assay was performed as previously described (Zendrini et al., 2019). Briefly, EVs were resuspended in 100 μl of PBS. Two microlitre of EV solution were resuspended in 23 μl of water, mixed with 50 μl of AuNPs 6 nM and 25 μl of PBS. The result of the assay was collected on Ensight MultiMode Reader (Perkin Elmer). When mixed with pure EV formulations, the AuNPs cluster on the EV membrane, whereas in EV formulations that contain soluble protein contaminants the AuNPs are preferentially cloaked by such proteins, which prevents AuNPs from clustering to the EV membrane. When AuNPs cluster, their localized surface plasmon resonance (LSPR) peak shifts and broadens, resulting in a colour change of the AuNP solution from red to blue, which can be accurately monitored through UV-Vis spectroscopy. AuNP

aggregation and therefore sample purity are described by the aggregation index ratio (AI%), a numerical value extrapolated from the UV-VIS spectra of the samples tested with the CONAN assay.

2.3.3 | SDS-PAGE and WB

EV samples were resuspended in Laemmli buffer and boiled at 95°C for 5 min, before being separated on a 10% polyacrylamide gel. Thirty μg of proteins were loaded for each sample. Proteins were then transferred onto a polyvinylidene difluoride (PVDF) membrane (GE Healthcare) for immunoblotting and blocked with 5% (w/v) fat-free dried milk in PBS 0.05% Tween-20(PBST) for 1 h at 37°C. Membranes were incubated overnight at 4°C with primary antibodies diluted in PBST 1% (w/v) fat-free dried milk. Membranes were washed 3 times in PBST and incubated with the HRP-conjugated secondary antibodies in PBST 1% (w/v) fat-free dried milk for 1 h at RT. After three washes, chemiluminescence was acquired using Bio-Rad Clarity Western ECL on a G:Box Chemi XT Imaging system (Syngene) (Alvisi et al., 2018). Primary antibodies used: sheep anti-human Antithrombin III (ATIII) (Hematologic Technologies INC, PAHAT-S), rabbit anti-Adam10 (Origene, AP05830PU-N), mouse anti-Alix (Santa Cruz, sc-53539), mouse anti-CD63 (Millipore, CBL553), mouse anti-CD81 (Santa Cruz, sc-7637), mouse anti-Tsg101 (Santa Cruz, sc-7964), rabbit anti-ApoI (Thermofisher, 701239), and mouse anti-GM130 (BD Bioscience, 610823). Secondary antibodies used: rabbit anti-mouse (Bethyl, A90-117P), donkey anti-sheep (Bethyl, A130-100P), and goat anti-rabbit (Bethyl, A120-101P). Primary antibodies were diluted 1:1000 except for sheep anti-human ATIII (1:3000). Secondary antibodies were diluted 1:3000.

2.3.4 | Dot blot assay and trypsin treatment

Dot blot was performed as previously described (Lai et al., 2015). Briefly, EVs were resuspended in 100 μl of 100 mM Tris, 150 mM NaCl, 1 mM EDTA. Five microlitre (*circa* 2 μg of EV-related proteins) of EVs diluted 1:1, 1:2, and 1:5(v/v) in buffer were spotted on a nitrocellulose membrane and allowed to dry at RT for 1 h. Membranes were then blocked with 5% (w/v) fat-free dried milk in Tris-buffered saline (TBS) in the absence or presence of 0.1% (v/v) Tween-20 for 1 h at RT, followed by the incubation overnight at 4°C with anti-CD63, anti-Ago2(Origene, TA352430) and anti-AT antibodies, diluted 1:1000 in TBS or TBST 1% fat-free dried milk. After three washes with TBS or TBST, membranes were incubated with HRP-conjugated with proper secondary antibodies diluted in TBS or TBST 1% fat-free dried milk for 1 h at RT. Blots were detected as described above. EV samples were also treated with 0.25% trypsin and incubated for 10 min at 37°C. Trypsin was inactivated by diluting the sample with PBS to 1 ml final volume. Samples were then centrifuged at 100,000 *g* for 2 h. The pellet and supernatant were dotted on the nitrocellulose membrane, as just described. The membranes were incubated with or without 0.1% (v/v) Tween-20.

2.3.5 | TCA-DOC/Acetone purification

To precipitate proteins and remove contaminants, plasma and EV samples were incubated at RT with 2% Na deoxycholate (DOC) (0.02% final concentration) and then with 10% trichloroacetic acid (TCA) for 15 min and 1 h, respectively. Samples were centrifuged at 20,000 *g* for 10 min at 4°C, then 200 μl of ice-cold acetone was added, incubating the sample on ice for 15 min. The centrifugation step was repeated and the resulting pellet was dried by inversion. Samples were finally resuspended with 350 μl of Rehydration buffer (Urea 7 M, Thiourea 2 M, CHAPS 4% (w/v), Carrier Ampholyte 0.5% (v/v), DTT 40 mM, Bromophenol Blue 0.002%), for the following 2D-PAGE.

2.3.6 | 2D-PAGE

For the isoelectrofocusing (IEF) phase, immobilized pH gradient (IPG) strips of 18 cm having a pH range four to seven (Ready Strips, Bio-Rad) were used and were rehydrated overnight at RT, adapting from Kremser et al. (2003). IEF was then performed on a Multiphor II Electrophoresis System with ImmobilineDryStrip Kit (Amersham Biosciences, Ge Healthcare), in four consecutive steps: (1) 1 min at 500 V, 1 mA, 5 W; (2) 1 h at 500 V, 1 mA, 5 W; (3) 4 h at 3500 V, 1 mA, 5 W; (4) 13.30 h at 3500 V, 1 mA, 5 W. Thirty microgram of proteins were loaded on each strip. After IEF, strips were equilibrated at RT under gently mixing with two different solutions of Equilibration buffer (SDS 2% (w/v), Urea 36% (w/v), 50 mM Tris-HCl pH 8.4, Glycerol 30% (v/v)) with DTT 2% (w/v) and iodoacetamide 2.5% (w/v), for 12 and 5 min, respectively. Strips were then frozen. Subsequently, strips were cut and the 6 cm piece with a pH range of five to six was inserted on the top of 8% SDS-PAGE gel and sealed with hot agarose solution (0.5% agar and Bromophenol Blue in Running buffer 1X). Electrophoresis and subsequent WB were performed as described above.

2.4 | Antithrombin activity on EVs

AT activity on EVs was evaluated by monitoring the formation of thrombin-antithrombin complex (TAT complex), as shown in literature (Martinez-Martinez et al., 2010). Briefly, ~1.5 ng of AT from plasma EV samples were incubated with 0.06 U of heparin for 30 min at 37°C. Then, the aliquots were mixed with 0.0025 U of thrombin and incubated at different timepoints (30 min, 1 h, 2 h, 4 h). Reactions of TAT complex formation were blocked adding Laemmli buffer 6X to each vial and boiling them at 95°C for 5 min. These samples were evaluated by 8% SDS-PAGE gel and subsequent WB, as indicated previously. The reaction was performed in triplicate on EVs from a pool of healthy subjects. Significant differences in TAT complex formation at different timepoints were determined with one-way ANOVA. P-values < 0.05 were considered statistically significant, with $^{*}P < 0.05$, $^{**}P < 0.01$, $^{***}P < 0.001$, and $^{****}P < 0.0001$. Values are shown as mean ± SD of three independent experiments.

2.5 | EV track

All relevant data has been submitted to the EV-TRACK knowledgebase (Van Deun et al., 2017). EV track ID: EV21008.

3 | RESULTS

3.1 | Antithrombin is associated to plasma small EVs

To separate and purify EVs from plasma, we performed differential (ultra)-centrifugations, followed by purification through a discontinuous sucrose gradient (Grossi et al., 2020) as shown in Figure 1.

Figure 2a shows a representative WB of the 12 fractions obtained from the gradient performed on a pool of healthy plasma samples. To verify the presence of EVs, common EV markers as Tsg101, CD63 and CD81(Thery et al., 2018) were probed. The negative marker GM130, was analyzed to exclude cellular contamination in the samples, and ApoAI, the specific marker for HDL lipoproteins, was checked to verify the presence of HDLs in the sample.

Thanks to this purification protocol, we could observe an enrichment of EVs in fractions six to nine (with density ranging from 1.11 and 1.22 g/cm; Danielsson & Bjork, 1982), with CD63 marker showing a shift towards heavier density fractions probably due to EV heterogeneity. GM130 is absent in all fractions, meaning that our samples do not contain any cellular contaminants. AT is enriched from fractions four to nine, overlapping the main EV markers. Recent studies demonstrated that the fraction with a density of 1.09 g/cm (Danielsson & Bjork, 1982) (corresponding in our gel to fraction five) may contain protein macro-aggregates or ectosomes, vesicles with a cellular origin that incorporate the coagulation factors released by platelets and endothelial cells (Sadallah et al., 2011).

The sucrose gradient allowed us to evidence that, by our experimental protocol and as shown earlier (Onodi et al., 2018), HDLs are mostly excluded from EV enriched fractions: they are present in fractions three to five and are particularly abundant in fraction four (with a density of 1.07 g/cm; Danielsson & Bjork, 1982), comparable with the density of the most abundant HDL types (Karimi et al., 2018). Gradient fraction four shows that AT is also present in HDL fractions: it might suggest that AT circulates in blood not only associated with EVs but also with HDLs. Afterwards, fractions six to nine were pooled and used for the subsequent analysis steps, being the fractions most enriched in EVs and deprived in HDLs.

Pooled particles from fractions six to nine were then imaged. AFM was employed to verify the presence of EVs in the pooled selected fractions (six to nine) and to visualize their morphology and size (Berardocco et al., 2017; Paolini, Orizio et al., 2018). Round-shaped objects with diameters ranging from 20 to 170 nm (Figure 2b) are visible in all the fractions tested. According to the size distribution analysis (Figure 2c) performed, most of the particles (~95%) are comprised in the 30–180 nm range, which is compatible with the size of small EVs. Objects featuring a size <30 nm are almost absent (<5%), further confirming the content of smaller biogenic particles of the fractions (e.g., HDLs, often co-isolated with small EVs) is negligible. To verify that our EV preparation was devoid of significant amount of protein contaminants, so to exclude free AT was not present as a soluble protein, we performed a colorimetric nanoplasmonic (CONAN) assay (Zendrini et al., 2019) As shown in Figure 2c, the AI% of the tested sample (green) falls below the LOD of the assay, highlighting that the content of free proteins in the sample is negligible (<20 ng/μl), thus indicating the isolation protocol used allows to obtain pure EV preparations.

To confirm that AT is present on EVs and that this finding is not dependent on the separation method used (Busatto et al., 2018), we have also performed the separation of EVs by SEC. As seen in Figure S1, AT is present in EV fractions eluted from SEC together with EV markers Adam 10 and CD81.

Taken together these results show that AT can circulate in blood on EVs and not only in a soluble free form (Kumar & Ragg, 2008).

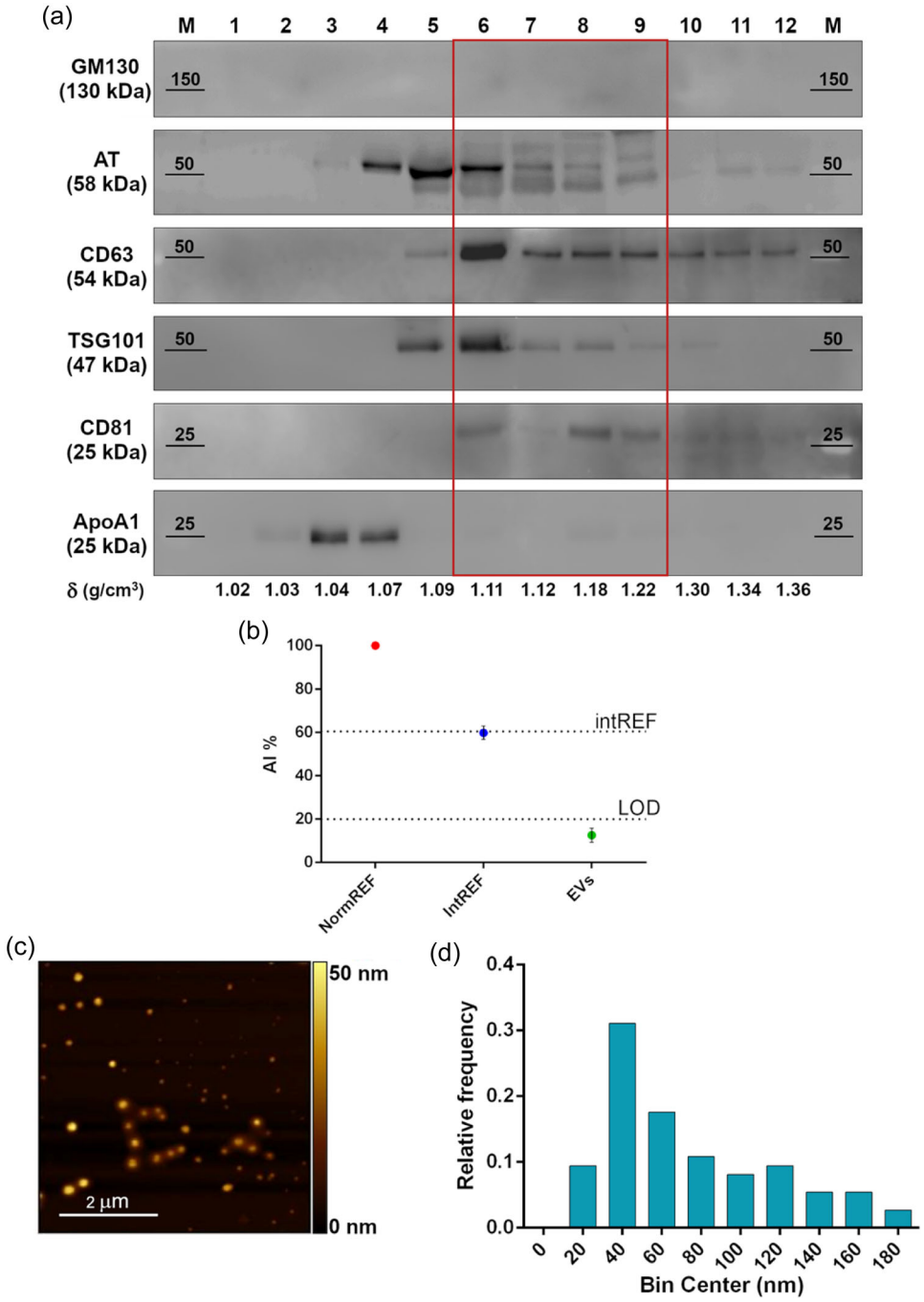

FIGURE 2 Comprehensive characterization of healthy plasma pool derived EVs. (a) Western blot analysis after SDS-PAGE of sucrose gradient fractions in reducing conditions. The distribution of EV (CD63, TSG101, CD81), Golgi (GM130, negative control), and lipoprotein (ApoA1, contaminant) markers is shown, together with AT. Fractions from 6 to 9, highlighted by the red rectangle, feature the absence of contaminants and the co-localization of AT and EV markers. (b) CONAN assay performed on the EV samples indicate that the isolation method used allows to obtain EV preparation with negligible amounts of soluble protein contaminants (soluble AT included). AI% value of a representative EV sample (green spot) is showed, together with assay internal controls (red and blue dots). (c) Representative AFM image of the particles in fractions six to nine, displaying intact and round shape objects, and a size comparable to the one of EV dried on a surface. (d) Size distribution of the particles in fractions six to nine, imaged through AFM. Particle diameter was extrapolated from 200 objects

We next performed a semi-quantitative analysis to estimate the levels of AT associated to EVs.

Figure 3a reports a representative WB of AT in plasma at different dilutions (lanes one to four) and EV-bound AT ("EVs" lane). AT content was related to the corresponding band intensity in plasma standards (lanes 1–4). Finally, we plotted a calibration line (Figure 3b, blue dots) and used it to estimate the amount of AT contained in the EV sample (Figure 3b, red star). The plotted value of each standard corresponds to the mean plasma AT content calculated from the maximum and the minimum plasma AT content reported in literature (Tsuchida et al., 2022). From our calculations, it appears that the amount of AT physiosorbed

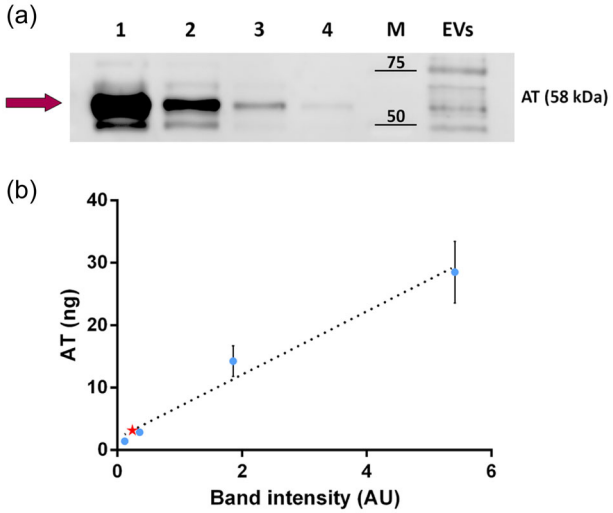

FIGURE 3 Semi-quantitative analysis of AT concentration on EVs. (a) EV-bound AT was measured using Western blot. Diluted plasma samples were used as standards. Lanes from 1 to 4 contain a diluted amount of plasma. Total protein loaded: 12.74 μg in lane 1; 6.37 μg in lane 2; 1.27 μg in lane 3; 0.64 μg in lane 4. The "EVs" lane was loaded with 1.41 μg of proteins, corresponding to the EVs separated from 160 μl of plasma. AT band (58 kDa) is highlighted by the purple arrow. (b) The calibration line created by plotting and linearly fitting ($R^2 = 0.9488$) the amount of AT calculated for plasma loaded in lanes 1–4 versus the corresponding band intensity measured through densitometric analysis. Blue dots: diluted plasma samples (Mean ± SD plotted). Red star: EV sample

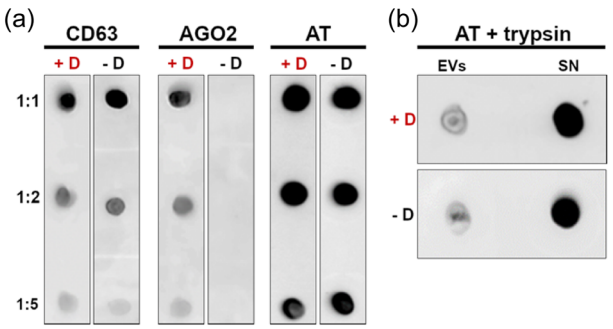

FIGURE 4 Analysis of AT localization onto EVs. EVs from plasma samples of healthy donors were spotted on nitrocellulose membrane and analyzed with dot-blot. All the tests were performed in presence (+D) and absence (-D) of 0.1% (v/v) Tween-20. Shown is a representative image of one of the three experiments performed. (a) Immunoblot vs. CD63 (EV membrane-associated protein), Ago2 (lumen protein), and AT in presence and absence of 0.1% (v/v) Tween-20. Membrane protein (CD63) signal is not affected by the detergent, while EV lumen protein (Ago2) is revealed only when the EV membrane is disrupted. The behaviour of AT suggests the association with EV membrane rather than its encapsulation within EV lumen. (b) Immunoblot versus AT performed on plasma EVs and supernatant after trypsin treatment and in presence (+D) or absence (-D) of 0.1% (v/v) Tween-20. Supernatant enriches in AT after trypsin treatment, meaning AT is directly accessible to the protease action, and further suggesting its localization on the outer leaflet of EV membrane

on the EVs separated from 1 ml of plasma is ~19.68 ng, that corresponds to ~ 0.02% of the mean total AT contained in 1 ml of human plasma (including free circulating AT and particle associated AT).

3.2 | AT is localized at the EV surface

AT is known to be a secreted soluble protein circulating in the blood; our evidences highlight it is also associated with EVs.

To characterize the nature of this interaction, a dot blot analysis with and without detergents has been performed. The technique consists of spotting purified EVs onto a nitrocellulose membrane at different dilutions. Afterwards, a WB is performed. Under these experimental conditions, if the vesicular protein is exposed to the solvent, it should be detected in the presence or absence of a detergent (which disrupts the membranes and allows the inner proteins to spread in the solution). As opposite, if the protein is contained inside the vesicles, it should be detected only in the presence of the detergent (Mckenzie et al., 2016; Paolini, Zendrini et al., 2018). Argonaute (Ago), being a protein present within the EVs, has been used as a negative control in this experiment. As shown in Figure 4a, only blots immunolabeled in the presence of the detergent revealed Ago2 signals when

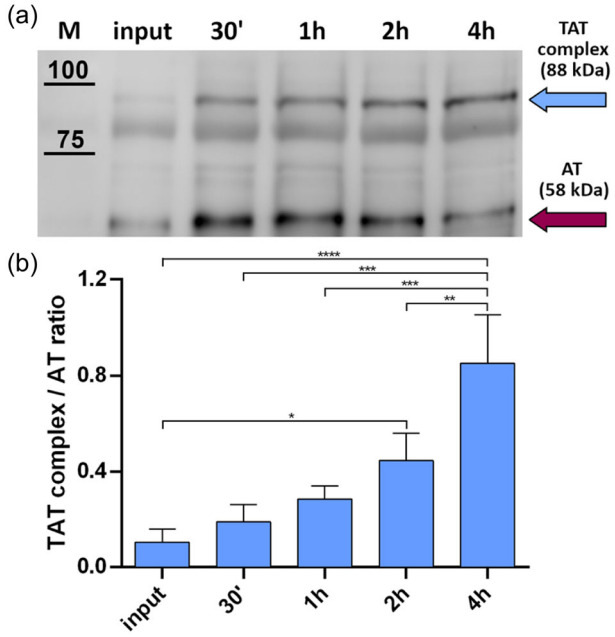

FIGURE 5 Determination of AT anticoagulant activity. EV-bound AT activity was assessed through the formation of the TAT complex. Fixed amounts of EVs (carrying ~1.5 ng of AT) were challenged with 0.06 U of heparin and 0.0025 U of thrombin. A representative image of three experiments is shown, together with the calculation of TAT complex and AT ratio by densitometric analysis. (a) TAT complex formation was measured at different timepoints through Western blot. Cyan arrow = TAT complex band. Purple arrow = AT band. (b) Normalized TAT complex/AT ratio at different timepoints. For each timepoint, the TAT complex band intensity was normalized on the respective AT band intensity (posed equal to 1). The input corresponds to TAT complex/AT ratio at T = 0 min. The displayed values represent the mean ± SD of three independent experiments. Significant differences in TAT complex formation at different timepoints were determined with one-way ANOVA test. *P*-values <0.05 were considered statistically significant. $^{*}P < 0.05$, $^{**}P < 0.01$, $^{***}P < 0.001$, and $^{****}P < 0.0001$

compared with the control (without detergent). On the contrary, the positive control CD63 was detected on both membranes treated or not with detergent. This EV marker is a transmembrane protein detected on the surface of EVs.

Results obtained with this experiment indicate that AT is localized in the EV membrane facing outwards since antibody anti-AT recognizes the epitope located outside of the vesicles, hence it cannot be an internal protein of EVs.

To verify whether AT could be detached from the EV membranes, EVs have been treated with an excess of trypsin (Figure 4b). Trypsin is a serine protease that hydrolyses proteins cleaving peptide chains mainly at the carboxyl side of the amino acid lysine or arginine. This treatment should detach and cleave the proteins linked or accessible in the vesicle membrane, releasing them in the extra-vesicular medium (Choi et al., 2020). Purified EVs from the sucrose gradient fractions were resuspended in a specific buffer with the addition of trypsin. After incubation and separation by UC, the pellet and supernatant were then dotted on the nitrocellulose membrane by applying the protocol described. As shown in Figure 4b, AT is mostly present in the supernatant fraction, meaning that trypsin has digested the protein and released it in solution. This observation corroborates the findings described above, suggesting that AT localizes at EV surface.

3.3 | AT on EVs retains anticoagulant activity

To determine if EV-AT retains anticoagulant activity, we evaluated the formation of a thrombin–antithrombin (TAT) complex in vitro as reported earlier (Martinez-Martinez et al., 2010). As shown from a representative image (Figure 5a) and from the histogram, which reports the formation of TAT complex at 37°C in presence of heparin and thrombin at different time-points (Figure 5b), we show a significant increase of TAT complex formation with time, with a corresponding consumption of free AT. It was interesting to notice that EVs separated from plasma already show the presence of TAT complex, presumably due to a scavenging property of EVs in blood.

3.4 | Specific AT glycoforms are enriched at the surface of EVs

Since the partitioning of plasma proteins in blood seems to be influenced by glycosylation (Kailemia et al., 2018), but no reported studies have compared EV glycosylation to the matched plasma, we verified if all the different glycoforms of AT circulating

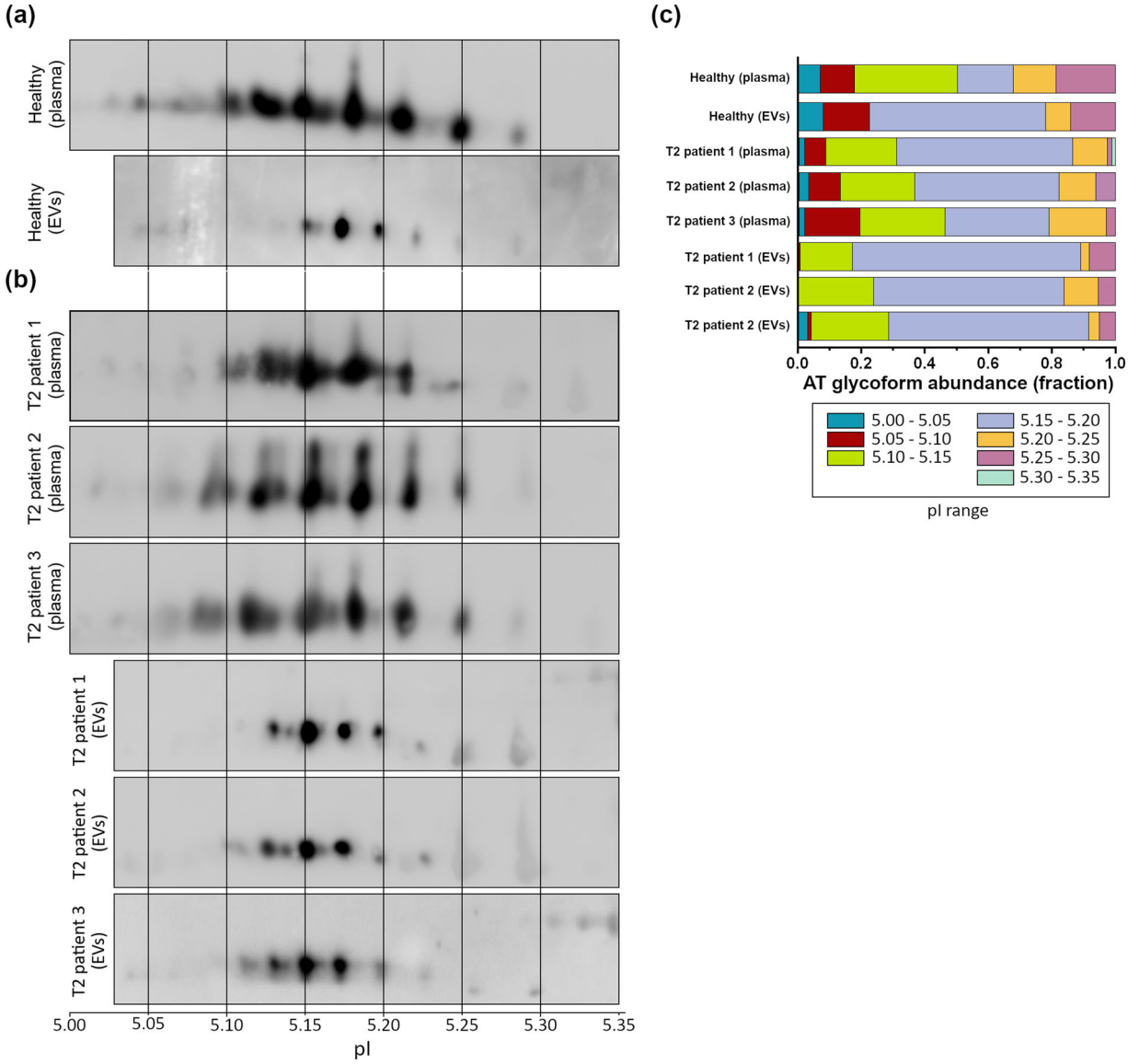

FIGURE 6 2D SDS-PAGE in reducing conditions on total plasma and isolated EV samples. (a) Comparison of the 2D profile of soluble AT in total plasma (above) and EV-associated AT (below), both derived from samples of healthy subjects. pI is indicated. The number of spots is considerably different from plasma to EVs, suggesting a degree of "EV-specificity" of some AT glycoforms. (b) 2D SDS-PAGE of whole plasma and EV-associated AT derived from three T2 patients, showing a different migration pattern of the AT-EVs in respect to the control healthy sample. (c) Densitometric analysis of the spots of soluble and EV-associated AT of healthy subjects and T2 patients. Differences in the relative abundance of AT glycoforms have been highlighted both in soluble and EV-associated AT of healthy subjects and in EV-associated AT of healthy subjects and T2 patients

in plasma are also associated with EVs. To compare total AT and EV-AT glycoforms we performed a 2D SDS-PAGE followed by WB on whole plasma pooled from five healthy subjects and on isolated EV samples (gradient fractions six to nine), both derived from the same pooled five healthy subjects. Comparing the 2D electropherograms we could observe different patterns (Figure 6a). Plasma AT exhibits a particular pattern composed of many spots at different intensities, similar to what has been shown for purified soluble AT (Kremser et al., 2003). EV-AT pattern shows instead a different profile: the overall number of spots (glycoforms) is lower and there seems to be specificity in binding for certain glycoforms with respect to others. In particular, glycoforms between 5.05 and 5.15 in pI units are almost absent in EVs. Furthermore, it is recognizable the presence of spots belonging to the group of β-AT isoforms (pI between 5.25 and 5.3). Overall, this pattern is not due to the total amount of loaded proteins but to a selective adsorption of those isoforms as evidenced in Figure 6c by the elaboration of densitometric profile of the AT spots of total AT and EV-AT, reporting relative abundances of AT glycoforms at different pIs intervals.

3.5 | EV associated AT shows a different 2D pattern between healthy and T2 patients

Given that specific AT glycoforms selectively associate with EVs in healthy subjects, we verified if a known mutation in AT coding sequence could lead to different AT adsorption patterns to EVs. We follow the hypothesis that mutations in the primary sequence of AT might lead to conformational changes in the structure of the enzyme, eventually altering the AT glyco-profile (Martinez-Martinez et al., 2010), thereby influencing its adsorption to the EV surface (De La Morena-Barrio et al., 2016; Mccoy et al., 2003).

We first performed a 2D SDS-PAGE of whole plasma from three T2 patients (all undergoing anticoagulant therapy), bearing the AT rare mutation R393C Northwick Park, which involves a reactive site defect (Figure 6b), followed by WB versus AT.

By comparing the spot profile and the relative plasma AT densitometric profile of patients with healthy subjects, we could appreciate at a glance only qualitative differences in spot distribution, which are better visualized in the densitometric profile, especially in the 5.15–5.20 pI range (Figure 6c). We next performed the WBs of EV-AT of the three EV samples isolated from the same patients' plasma. By looking at WB, we could well appreciate differences in AT isoforms adsorption with a higher number of EV-AT spots bearing a more acidic pI in T2 samples respect to controls (healthy EVs, Figure 6a). In particular, the pI interval between 5.10 and 5.15 shows two to four spots that are not present in EVs from controls. The differences are also well evidenced in the elaboration of the densitometric profile shown in Figure 6c.

4 | DISCUSSION

In the past few years, it has become clearer and clearer that EV surface molecules are of critical functional significance (Buzas et al., 2018) since they allow to establish connections with cells (Di Noto et al., 2014) and with other biogenic nanoparticles in biological fluids (Busatto et al., 2020). EV surface molecules comprise integral, peripheral, and lipid-anchored membrane proteins, but also an extravesicular cargo of proteins adsorbed to EVs, at least partly recruited in body fluids after vesicle shedding (Rai et al., 2021).

We might assume that only few of the proteins on EV surface are recruited during vesicle biogenesis and/or release by the producing cell. Indeed, as demonstrated for synthetic nanoparticles (Busatto et al., 2019), EVs are able to recruit on their surface numerous proteins which are present in circulation. The nature of such "protein corona" has recently started to be investigated as for other biogenic nanoparticles (Asztalos et al., 2011; Buzas et al., 2018; Paolini, Orizio et al., 2018; Toth et al., 2021; Wolf et al., 2022; Yerneni et al., 2021). Such investigation promises to disclose new properties of EVs since EV protein corona might be involved in EV-mediated cellular communication or can even provide EVs with new regulatory functions.

In this proof of concept study we provide strong evidence that active AT is part of the protein corona of EVs with a composition modulated by glycosylation. First, we have evidenced AT is effectively present on EVs, by applying serial ultra-centrifugation followed by sucrose density gradient, which allowed us to confirm the presence of the protein on-board. Since by bioinformatic predictions and literature data AT is not predicted to be a membrane-anchored protein and it is normally shed into the circulation by hepatocytes by transport along the exocytotic pathway (Vogel & Larsen, 2000), we verified its association to EVs by dot blot analysis. This technique confirmed that AT shows an exofacial topology and it is indeed detachable by treatment with trypsin (Choi et al., 2020). We next verified that physiosorbed EV-AT still retains activity evaluating the formation of the TAT complex in vitro. Not surprisingly, but never shown before, we noticed that EVs already carry the TAT complex on their surface, suggesting a role for EVs of "scavenger" bio-nanoparticles. Moreover, we wanted to quantify how much AT travels physiosorbed to EVs, and we have shown that around 0.02%of the whole plasma AT is effectively and actively travelling on EVs.

As mentioned earlier, AT can be modified by N-glycosylation (Picard et al., 1995), and this PTM is important for its function as anticoagulant agent, probably altering its interaction with heparin (De La Morena-Barrio et al., 2016; Mccoy et al., 2003; Yamada et al., 2016). Glycosylation is the only PTM of the protein and no other modification has been reported in literature (Kremser et al., 2003). Glycosylation has also been evidenced to have a role in recruiting proteins to HDLs (Kailemia et al., 2018), hence we verified if this PTM could also play a role in the adsorption process of AT to EVs.

By performing 2D-SDS PAGE, which allows discriminating the different glycoforms of AT, we have evidenced for the first time that not all AT glycoforms are equally adsorbed to EV surface, and some are more favoured for EV recruitment, indicating glycan specificity in recruiting AT onto EVs. By comparing the spot profile of EV-AT isoforms with previous published data (Kremser et al., 2003) we suggest that both α-AT isoforms and β-AT isoforms are present on EVs, even if at different ratio in respect to plasma. In particular, highly sialylated isoforms (5.05-5.15 in pI units) are almost absent on EVs. This is the first observation that a protein is specifically attached to the EV surface based on its glycosylation, although others have shown that glycosylation is important for EV biodistribution (Royo et al., 2019) and functions (Williams et al., 2018).

We believe that studying the selectivity of adsorption of AT glycoforms to EVs could be of importance to unravel hidden roles of AT in the coagulation process (Águila et al., 2021). EVs could indeed offer a surface to accelerate the anticoagulant effect of AT in circulation, as it happens for vascular endothelium heparan sulfates (Patnaik & Moll, 2008), or bring a local anti-inflammatory effect.

Notably, AT can be defined as a very "sticky" protein since it has also been found attached to the surface of HDLs (Gordon et al., 2010; Vaisar et al., 2007), conferring these lipoproteins a direct role in coagulation that has not yet been investigated, and as protein corona component of PEG-liposomes after incubation with fetal bovine serum under dynamic and static conditions (Palchetti et al., 2016). Since AT glycosylation has not been considered in these cited literature results, we might assume that a signature of specific AT glycoforms can be found on the protein corona of HDLs and synthetic liposomes, bringing along diagnostic and therapeutic implications.

In order to highlight possible future clinical implications of those findings, we further analyzed whole plasma and EV-AT 2D electrophoretic profile in three patients affected by AT T2 deficiency, caused by a R393C mutation in the primary sequence of AT. This mutation is known to alter the formation of a hydrogen bond in the structure of the serpin, thus leading to higher K_d for heparin. No other mutations nor glycosylation alterations have earlier been described associated with this mutation. As evidenced by our 2D analysis, interestingly, whole plasma AT from T2 patients has a slight different spot profile compared to healthy controls, probably because the mutation R393C does influence AT glycoprofile in some ways, which have to be demonstrated. Furthermore, this different glycoprofile is much more evident in EV-AT electropherogram showing that specific isoforms are adsorbed onto EVs in respect to controls, with a prevalence of more acidic glycoforms adsorbed to EVs in T2 patients (Figure 6b). Hence, we hypothesize AT glycans are involved in the selective adsorption of AT to EVs.

All together this data suggests that analysis of AT-EVs but in general analysis of EV protein corona, brings about another "dimension," that is, EV adsorption capacity, in our case related to glycosylation, which can better help to visualize protein alterations that could be neglected by analysing whole plasma.

5 | CONCLUSIONS

This study proofs that some active AT travels physiosorbed on the surface of plasma EVs, contributing to form the "EV-protein corona." The corona is enriched in specific AT glycoforms, thus suggesting glycosylation to play a key role in AT partitioning between EVs and plasma. Differences in AT glycoform composition of the corona of EVs separated from plasma of a small cohort of healthy and AT qualitative deficiency-affected subjects were also identified, as previously demonstrated for HDL related pathologies (Krishnan et al., 2017).

Assessment of this proof-of-concept results with a statistically significant cohort of patients, will tell us if these findings set the base for a new diagnostic test based on EVs to identify AT deficiency subtypes. This is highly desirable, as current methods to measure levels of functional AT make use of synthetic substrate technology (Goodnight et al., 1980) bearing many limitations ascribable to the type of synthetic peptide employed and to substrate cleavage by contaminant proteases. Moreover, no functional routine diagnostic assay can be assumed to detect all forms of AT deficiencies since false-negative results may hamper the diagnosis.

This diagnostic limitation also hampers the prognosis since different AT deficiency subtypes may have a lower risk of thrombosis. EV-based AT test would allow to get around this limitations being not a functional but rather a test based on AT biophysical properties.

On a wider perspective. this work provides further proof that dissecting the plasma into its nanostructured components and the interaction among them, such as the EVs and their protein corona, is a challenging but very fruitful approach to understand physiological and pathological role of proteins in the extracellular environment, including the elusive disorders related to post-translational defects (e.g., congenital disorders of glycosylation).

AUTHORSHIP CONTRIBUTIONS

Conceptualization: Annalisa Radeghieri, Doris Ricotta. Investigation: Annalisa Radeghieri, Silvia Alacqua, Francesca Todaro, Vanessa Previcini, Andrea Zendrini. Resources: Giuliana Martini. Writing – Original Draft: Annalisa Radeghieri, Silvia Alacqua, Andrea Zendrini. Writing- Review & Editing: All authors. Visualization: Andrea Zendrini. Supervision: Annalisa Radeghieri, Paolo Bergese. Project administration: Annalisa Radeghieri. Funding acquisition: Annalisa Radeghieri, Paolo Bergese. Please turn to the CRedit taxonomy for the term explanation.

ACKNOWLEDGEMENTS

This research was supported the University of Brescia through "Fondo per la ricerca ex 60%", by MIUR through PRIN 2017E3A2NR_004 project and by the Center for Colloid and Surface Science (CSGI), Florence through internal funds.

CONFLICTS OF INTEREST

No potential conflict of interest was reported by the authors. We thank Lucia Paolini, Giuseppe Pomarico and Valerio De Stefano for helpful discussions.

ORCID

Annalisa Radeghieri https://orcid.org/0000-0003-2737-1090

REFERENCES

Águila, S., Noto, R., Luengo-Gil, G. S., Espã-N, S., Bohdan, N., De La Morena-Barrio, M. A. E., Peñs, J., Rodenas, M. C., Vicente, V., Corral, J., Manno, M., & Martã-Nez-Martã-Nez, I. (2021). N-glycosylation as a tool to study antithrombin secretion, conformation, and function. *International Journal of Molecular Sciences*, *22*(2), 516.

Alvisi, G., Paolini, L., Contarini, A., Zambarda, C., Di Antonio, V., Colosini, A., Mercandelli, N., Timmoneri, M., Palã[1], G., Caimi, L., Ricotta, D., & Radeghieri, A. (2018). Intersectin goes nuclear: Secret life of an endocytic protein. *The Biochemical Journal*, *475*(8), 1455–1472. https://doi.org/10.1042/BCJ20170897

Asztalos, B. F., Tani, M., & Schaefer, E. J. (2011). Metabolic and functional relevance of HDL subspecies. *Current Opinion in Lipidology*, *22*(3), 176–185. https://doi.org/10.1097/MOL.0b013e3283468061

Atay, S., Gercel-Taylor, C., Kesimer, M., & Taylor, D. D. (2011). Morphologic and proteomic characterization of exosomes released by cultured extravillous trophoblast cells. *Experimental Cell Research*, *317*(8), 1192–1202. https://doi.org/10.1016/j.yexcr.2011.01.014

Berardocco, M., Radeghieri, A., Busatto, S., Gallorini, M., Raggi, C., Gissi, C., D'Agnano, I., Bergese, P., Felsani, A., & Berardi, A. C. (2017). RNA-seq reveals distinctive RNA profiles of small extracellular vesicles from different human liver cancer cell lines. *Oncotarget*, *8*, 82920–82939. 10.18632/oncotarget.20503

Busatto, S., Vilanilam, G., Ticer, T., Lin, W.-L., Dickson, D., Shapiro, S., Bergese, P., & Wolfram, J. (2018). Tangential flow filtration for highly efficient concentration of extracellular vesicles from large volumes of fluid. *Cells*, *7*(12), 273. https://doi.org/10.3390/cells7120273

Busatto, S., Yang, Y., Walker, S. A., Davidovich, I., Lin, W.-H., Lewis-Tuffin, L., Anastasiadis, P. Z., Sarkaria, J., Talmon, Y., Wurtz, G., & Wolfram, J. (2020). Brain metastases-derived extracellular vesicles induce binding and aggregation of low-density lipoprotein. *Journal of Nanobiotechnology*, *18*(1), 162. https://doi.org/10.1186/s12951-020-00722-2

Busatto, S., Zendrini, A., Radeghieri, A., Paolini, L., Romano, M., Presta, M., & Bergese, P. (2019). The nanostructured secretome. *Biomaterials Science*, *8*(1), 39–63. https://doi.org/10.1039/c9bm01007f

Buzas, E. I., Toth, E. A., Sodar, B. W., & Szabo-Taylor, K. E. (2018). Molecular interactions at the surface of extracellular vesicles. *Seminars in Immunopathology*, *40*, 453–464. https://doi.org/10.1007/s00281-018-0682-0

Choi, D., Go, G., Kim, D. K., Lee, J., Park, S. M., Di Vizio, D., & Gho, Y. S. (2020). Quantitative proteomic analysis of trypsin-treated extracellular vesicles to identify the real-vesicular proteins. *Journal of Extracellular Vesicles*, *9*(1), 1757209. https://doi.org/10.1080/20013078.2020.1757209

Dahlbaeck, B., Wiedmer, T., & Sims, P. J. (1992). Binding of anticoagulant vitamin K-dependent protein S to platelet-derived microparticles. *Biochemistry*, *31*(51), 12769–12777. https://doi.org/10.1021/bi00166a009

Danielsson, A., & Bjork, I. (1982). Mechanism of inactivation of trypsin by antithrombin. *The Biochemical Journal*, *207*(1), 21–28. https://doi.org/10.1042/bj2070021

De La Morena-Barrio, M. E., Martã-Nez-Martã-Nez, I., De Cos, C., Wypasek, E., Roldán, V., Undas, A., Van Scherpenzeel, M., Lefeber, D. J., Toderici, M., Sevivas, T., España, F., Jaeken, J., Corral, J., & Vicente, V. (2016). Hypoglycosylation is a common finding in antithrombin deficiency in the absence of a SERPINC1 gene defect. *Journal of Thrombosis and Haemostasis*, *14*(8), 1549–1560. https://doi.org/10.1111/jth.13372

Demelbauer, U. M., Plematl, A., Josic, D., Allmaier, G., & Rizzi, A. (2005). On the variation of glycosylation in human plasma derived antithrombin. *Journal of Chromatography A*, *1080*(1), 15–21. https://doi.org/10.1016/j.chroma.2005.01.057

Demelbauer, U. M., Plematl, A., Kremser, L., Allmaier, G., Josic, D., & Rizzi, A. (2004). Characterization of glyco isoforms in plasma-derived human antithrombin by on-line capillary zone electrophoresis-electrospray ionization-quadrupole ion trap-mass spectrometry of the intact glycoproteins. *Electrophoresis*, *25*(13), 2026–2032. https://doi.org/10.1002/elps.200305936

Di Noto, G., Chiarini, M., Paolini, L., Mazzoldi, E. L., Giustini, V., Radeghieri, A., Caimi, L., & Ricotta, D. (2014). Immunoglobulin free light chains and GAGs mediate multiple myeloma extracellular vesicles uptake and secondary NfkappaB nuclear translocation. *Frontiers in Immunology*, *5*, 517. https://doi.org/10.3389/fimmu.2014.00517

Donges, R., Romish, J., Stauss, H., & Brazel, D. (2001). Separation of antithrombin III variants by micellar electrokinetic chromatography. *Journal of Chromatography A*, *924*(1-2), 307–313. https://doi.org/10.1016/s0021-9673(01)00827-5

Franzen, L. E., Svensson, S., & Larm, O. (1980). Structural studies on the carbohydrate portion of human antithrombin III. *The Journal of Biological Chemistry*, *255*(11), 5090–5093.

Goodnight, S. H., Schaeffer, J. L., & Sheth, K. (1980). Measurement of antithrombin III in normal and pathologic states using chromogenic substrate S-2238. Comparison with immunoelectrophoretic and factor Xa inhibition assays. *American Journal of Clinical Pathology*, *73*(5), 639–647. https://doi.org/10.1093/ajcp/73.5.639

Gordon, S. M., Deng, J., Lu, L. J., & Davidson, W. S. (2010). Proteomic characterization of human plasma high density lipoprotein fractionated by gel filtration chromatography. *Journal of Proteome Research*, *9*(10), 5239–5249. https://doi.org/10.1021/pr100520x

Grossi, I., Radeghieri, A., Paolini, L., Porrini, V., Pilotto, A., Padovani, A., Marengoni, A., Barbon, A., Bellucci, A., Pizzi, M., Salvi, A., & De Petro, G. (2020). MicroRNA34a5p expression in the plasma and in its extracellular vesicle fractions in subjects with Parkinson's disease: An exploratory study. *International Journal of Molecular Medicine*, 533–546. https://doi.org/10.3892/ijmm.2020.4806

Kailemia, M. J., Wei, W., Nguyen, K., Beals, E., Sawrey-Kubicek, L., Rhodes, C., Zhu, C., Sacchi, R., Zivkovic, A. M., & Lebrilla, C. B. (2018). Targeted measurements of O- and N-glycopeptides show that proteins in high density lipoprotein particles are enriched with specific glycosylation compared to plasma. *Journal of Proteome Research*, *17*(2), 834–845. https://doi.org/10.1021/acs.jproteome.7b00604

Karimi, N., Cvjetkovic, A., Jang, Su C., Crescitelli, R., Hosseinpour Feizi, M. A., Nieuwland, R., Lötvall, J., & LÃ¤Sser, C. (2018). Detailed analysis of the plasma extracellular vesicle proteome after separation from lipoproteins. *Cellular and Molecular Life Sciences*, *75*(15), 2873–2886. https://doi.org/10.1007/s00018-018-2773-4

Kremser, L., Brückner, A., Heger, A., Grunert, T., Buchacher, A., Josic, D., Allmaier, G., & Rizzi, A. (2003). Characterization of antithrombin III from human plasma by two-dimensional gel electrophoresis and capillary electrophoretic methods. *Electrophoresis*, *24*(24), 4282–4290. https://doi.org/10.1002/elps.200305651

Krishnan, S., Shimoda, M., Sacchi, R., Kailemia, M. J., Luxardi, G., Kaysen, G. A., Parikh, A. N., Ngassam, V. N., Johansen, K., Chertow, G. M., Grimes, B., Smilowitz, J. T., Maverakis, E., Lebrilla, C. B., & Zivkovic, A. M. (2017). HDL glycoprotein composition and site-specific glycosylation differentiates between clinical groups and affects IL-6 secretion in lipopolysaccharide-stimulated monocytes. *Scientific Reports*, *7*, 43728. https://doi.org/10.1038/srep43728

Kumar, A., & Ragg, H. (2008). Ancestry and evolution of a secretory pathway serpin. *BMC Evolutionary Biology*, *8*, 250. https://doi.org/10.1186/1471-2148-8-250

Lai, C. P., Kim, E. Y., Badr, C. E., Weissleder, R., Mempel, T. R., Tannous, B. A., & Breakefield, X. O. (2015). Visualization and tracking of tumour extracellular vesicle delivery and RNA translation using multiplexed reporters. *Nature Communications*, *6*, 7029. https://doi.org/10.1038/ncomms8029

Lane, D. A., Bayston, T., Olds, R. J., Fitches, A. C., Cooper, D. N., Millar, D. S., Jochmans, K., Perry, D. J., Okajima, K., Thein, S. L., & Emmerich, J. (1997). Antithrombin mutation database: 2nd (1997) update. For the plasma coagulation inhibitors subcommittee of the scientific and standardization committee of the international society on thrombosis and haemostasis. *Thrombosis and Haemostasis*, *77*(1), 197–211.

Levin, G. Y., & Sukhareva, E. (2015). Antithrombin activity in microvesicles derived from stored red blood cells. *Blood Transfus*, *13*(4), 688–689. https://doi.org/10.2450/2015.0016-15

Luengo-Gil, G. S., Garcia, A. B., Ortega-Sabater, C., Bohdan, N., Espín, S., Peñas-Martínez, J., Martínez-Planes, E., García-Hernández, Ã., Vicente, V., Quintanilla, M., & Martínez-Martínez, I. (2019). Antithrombin is incorporated into exosomes produced by antithrombin non-expressing cells. *Biochimie*, *165*, 245–249. https://doi.org/10.1016/j.biochi.2019.08.010

Mammen, E. (1998). Antithrombin: Its physiological importance and role in DIC. *Seminars in Thrombosis and Hemostasis*, *24*(1), 19–25. https://doi.org/10.1055/s-2007-995819

Martinez-Martinez, I., Ordonez, A., Navarro-Fernandez, J., Perez-Lara, A., Gutierrez-Gallego, R., Giraldo, R., Martinez, C., Llop, E., Vicente, V., & Corral, J. (2010). Antithrombin Murcia (K241E) causing antithrombin deficiency: A possible role for altered glycosylation. *Haematologica*, *95*(8), 1358–1365. https://doi.org/10.3324/haematol.2009.015487

Mathieu, M., Martin-Jaular, L., Lavieu, G., & Théry, C. (2019). Specificities of secretion and uptake of exosomes and other extracellular vesicles for cell-to-cell communication. *Nature Cell Biology*, *21*(1), 9–17. https://doi.org/10.1038/s41556-018-0250-9

Mccoy, A. J., Pei, X. Y., Skinner, R., Abrahams, J. P., & Carrell, R. W. (2003). Structure of beta-antithrombin and the effect of glycosylation on antithrombin's heparin affinity and activity. *Journal of Molecular Biology*, *326*(3), 823–833. https://doi.org/10.1016/s0022-2836(02)01382-7

Mckenzie, A. J., Hoshino, D., Hong, N. H., Cha, D. J., Franklin, J. L., Coffey, R. J., Patton, J. G., & Weaver, A. M. (2016). KRAS-MEK signaling controls Ago2 sorting into exosomes. *Cell Reports*, *15*(5), 978–987. https://doi.org/10.1016/j.celrep.2016.03.085

Montis, C., Caselli, L., Valle, F., Zendrini, A., Carlã, F., Schweins, R., Maccarini, M., Bergese, P., & Berti, D. (2020). Shedding light on membrane-templated clustering of gold nanoparticles. *Journal of Colloid and Interface Science*, *573*, 204–214. https://doi.org/10.1016/j.jcis.2020.03.123

Morad-Rémy, M.-S., Saunderson, S. C., Dunn, A. C., Faed, J. M., Kleffmann, T., & Mclellan, A. D. (2016). Procoagulant and immunogenic properties of melanoma exosomes, microvesicles and apoptotic vesicles. *Oncotarget*, *7*(35), 56279–56294.

Murano, G., Williams, L., Miller-Andersson, M., Aronson, D. L., & King, C. (1980). Some properties of anti-thrombin-Iii and its concentration in human-plasma. *Thrombosis Research*, *18*(1-2), 259–262. https://doi.org/10.1016/0049-3848(80)90190-5

Nomura, S. (2017). Extracellular vesicles and blood diseases. *International Journal of Hematology*, *105*(4), 392–405. https://doi.org/10.1007/s12185-017-2180-x

Nomura, S., Ozaki, Y., & Ikeda, Y. (2008). Function and role of microparticles in various clinical settings. *Thrombosis Research*, *123*(1), 8–23. https://doi.org/10.1016/j.thromres.2008.06.006

Olson, S., & Bjork, I. (1994). Regulation of thrombin activity by antithrombin and heparin. *Seminars in Thrombosis and Hemostasis*, *20*(4), 373–409. https://doi.org/10.1055/s-2007-1001928

Onodi, Z., Pelyhe, C., Terezia Nagy, C., Brenner, G. B., Almasi, L., Kittel, A., Manček-Keber, M., Ferdinandy, P. T., Buzsa, E. I., & Giricz, Z. N. (2018). Isolation of high-purity extracellular vesicles by the combination of iodixanol density gradient ultracentrifugation and bind-elute chromatography from blood plasma. *Frontiers in Physiology*, *9*, 1479. https://doi.org/10.3389/fphys.2018.01479

Palchetti, S., Colapicchioni, V., Digiacomo, L., Caracciolo, G., Pozzi, D., Capriotti, A. L., La Barbera, G., & Laganã, A. (2016). The protein corona of circulating PEGylated liposomes. *Biochimica Et Biophysica Acta*, *1858*(2), 189–196. https://doi.org/10.1016/j.bbamem.2015.11.012

Paolini, L., Orizio, F., Busatto, S., Radeghieri, A., Bresciani, R., Bergese, P., & Monti, E. (2018). Exosomes secreted by HeLa cells shuttle on their surface the plasma membrane-associated sialidase NEU3. *Biochemistry*, *56*(48), 6401–6408. https://doi.org/10.1021/acs.biochem.7b00665

Paolini, L., Zendrini, A., & Radeghieri, A. (2018). Biophysical properties of extracellular vesicles in diagnostics. *Biomarkers in Medicine*, 383–391. https://doi.org/10.2217/bmm-2017-0458

Patnaik, M. M., & Moll, S. (2008). Inherited antithrombin deficiency: A review. *Haemophilia*, *14*(6), 1229–1239. https://doi.org/10.1111/j.1365-2516.2008.01830.x

Pérez-Casal, M., Downey, C., Fukudome, K., Marx, G., & Toh, C. H. (2005). Activated protein C induces the release of microparticle-associated endothelial protein C receptor. *Blood*, *105*(4), 1515–1522. https://doi.org/10.1182/blood-2004-05-1896

Persson, E., Bak, H., & Olsen, O. H. (2001). Substitution of valine for leucine 305 in factor VIIa increases the intrinsic enzymatic activity. *The Journal of Biological Chemistry*, *276*(31), 29195–29199. https://doi.org/10.1074/jbc.M102187200

Petersen, T. E. D.-W. G., & Sottrup-Jensen, L. (1979). Primary structure of antithrombin III (heparin cofactor): Partial homology between alpha 1 antitrypsin and antithrombin III. In: Collen, D W. B., & Verstraete, M. eds *The physiological inhibitors of blood coagulation and fibrinolysis*. Elsevier Science;:43–54.

Picard, V., Ersdal-Badju, E., & Bock, S. C. (1995). Partial glycosylation of antithrombin III asparagine-135 is caused by the serine in the third position of its N-glycosylation consensus sequence and is responsible for production of the beta-antithrombin III isoform with enhanced heparin affinity. *Biochemistry*, *34*(26), 8433–8440. https://doi.org/10.1021/bi00026a026

Rai, A., Fang, H., Claridge, B., Simpson, R. J., & Greening, D. W. (2021). Proteomic dissection of large extracellular vesicle surfaceome unravels interactive surface platform. *Journal of Extracellular Vesicles*, *10*(13), e12164. https://doi.org/10.1002/jev2.12164

Rikkert, L. G., Coumans, F. A. W., Hau, C. M., Terstappen, L. W. M. M., & Nieuwland, R. (2021). Platelet removal by single-step centrifugation. *Platelets*, *32*(4), 440–443. https://doi.org/10.1080/09537104.2020.1779924

Royo, F., Cossío, U., Ruiz de Angulo, A., Llop, J., & Falcon-Perez, J. M. (2019). Modification of the glycosylation of extracellular vesicles alters their biodistribution in mice. *Nanoscale*, *11*(4), 1531–1537. https://doi.org/10.1039/C8NR03900C

Sadallah, S., Eken, C., & Schifferli, J. A. (2011). Ectosomes as modulators of inflammation and immunity. *Clinical and Experimental Immunology*, *163*(1), 26–32. https://doi.org/10.1111/j.1365-2249.2010.04271.x

SC B. Antithrombin III and heparin cofactor II. *Hemostasis and thrombosis: Basic principles and clinical practice*. Lippincott Williams & Wilkins, (2001).

Thery, C., Witwer, K. W., Aikawa, E., Alcaraz, M. J., Anderson, J. D., Andriantsitohaina, R., Antoniou, A., Arab, T., Archer, F., Atkin-Smith, G. K., Ayre, D. C., Bach, J. M., Bachurski, D., Baharvand, H., Balaj, L., Baldacchino, S., Bauer, N. N., Baxter, A. A., Bebawy, M., … Zuba-Surma, E. K. (2018). Minimal information for studies of extracellular vesicles 2018 (MISEV2018): A position statement of the International Society for Extracellular Vesicles and update of the MISEV2014 guidelines. *Journal of Extracellular Vesicles*, *7*(1), 1535750. https://doi.org/10.1080/20013078.2018.1535750

Toth, E. A., Turiak, L., Visnovitz, T., Cserép, C., Mazlo, A., Sodar, B. W., Försönits, A. I., Petővári, G., Sebestyén, A., Komlosi, Z., Drahos, L., Kittel, A., Nagy, G. R., Bácsi, A., Denes, A., Gho, Y. S., Szabo-Taylor, K. E., & Buzas, E. I. (2021). Formation of a protein corona on the surface of extracellular vesicles in blood plasma. *Journal of Extracellular Vesicles*, *10*(11), e12140. https://doi.org/10.1002/jev2.12140

Tripisciano, C., Weiss, R., Eichhorn, T., Spittler, A., Heuser, T., Fischer, M. B., & Weber, V. (2017). Different potential of extracellular vesicles to support thrombin generation: Contributions of phosphatidylserine, tissue factor, and cellular origin. *Scientific Reports*, *7*(1), 6522. https://doi.org/10.1038/s41598-017-03262-2

Tsuchida, T., Hayakawa, M., Kawahara, S., & Kumano, O. (2022). Thrombin generation capacity is enhanced by low antithrombin activity and depends on the activity of the related coagulation factors. *Thrombosis Journal*, *20*(1), 29. https://doi.org/10.1186/s12959-022-00388-w

Vaisar, T., Pennathur, S., Green, P. S., Gharib, S. A., Hoofnagle, A. N., Cheung, M. C., Byun, J., Vuletic, S., Kassim, S., Singh, P., Chea, H., Knopp, R. H., Brunzell, J., Geary, R., Chait, A., Zhao, X.-Q., Elkon, K., Marcovina, S., Ridker, P., … Heinecke, J. W. (2007). Shotgun proteomics implicates protease inhibition and complement activation in the antiinflammatory properties of HDL. *The Journal of Clinical Investigation*, *117*(3), 746–756. https://doi.org/10.1172/JCI26206

Van Deun, J., Mestdagh, P., Agostinis, P., Akay, Ã. –Z., Anand, S., Anckaert, J., Martinez, Z. A., Baetens, T., Beghein, E., Bertier, L., Berx, G., Boere, J., Boukouris, S., Bremer, M., Buschmann, D., Byrd, J. B., Casert, C., Cheng, L., Cmoch, A., …, Hendrix, A. (2017). EV-TRACK: Transparent reporting and centralizing knowledge in extracellular vesicle research. *Nature Methods*, *14*(3), 228–232. https://doi.org/10.1038/nmeth.4185

Vogel, L. K., & Larsen, J. E. (2000). Apical and non-polarized secretion of serpins from MDCK cells. *FEBS Letters*, *473*(3), 297–302. https://doi.org/10.1016/s0014-5793(00)01548-9

Williams, C., Royo, F., Aizpurua-Olaizola, O., Pazos, R., Boons, G.-J., Reichardt, N.-C., & Falcon-Perez, J. M. (2018). Glycosylation of extracellular vesicles: Current knowledge, tools and clinical perspectives. *Journal of Extracellular Vesicles*, *7*(1), 1442985. https://doi.org/10.1080/20013078.2018.1442985

Wolf, M., Poupardin, R. W., Ebner-Peking, P., Andrade, A. C., Blöchl, C., Obermayer, A., Gomes, F. G., Vari, B., Maeding, N., Eminger, E., Binder, H. M., Raninger, A. M., Hochmann, S., Brachtl, G., Spittler, A., Heuser, T., Ofir, R., Huber, C. G., Aberman, Z., …, Strunk, D. (2022). A functional corona around extracellular vesicles enhances angiogenesis, skin regeneration and immunomodulation. *Journal of Extracellular Vesicles*, *11*(4), e12207. https://doi.org/10.1002/jev2.12207

Yamada, T., Kanda, Y., Takayama, M., Hashimoto, A., Sugihara, T., Satoh-Kubota, A., Suzuki-Takanami, E., Yano, K., Iida, S., & Satoh, M. (2016). Comparison of biological activities of human antithrombins with high-mannose or complex-type nonfucosylated N-linked oligosaccharides. *Glycobiology*, *26*(5), 482–492. https://doi.org/10.1093/glycob/cww001

Yerneni, S. S., Solomon, T., Smith, J., & Campbell, P. G. (2021). Radioiodination of extravesicular surface constituents to study the biocorona, cell trafficking and storage stability of extracellular vesicles. *Biochimica et Biophysica Acta - General Subjects*, *1866*(2), 130069. https://doi.org/10.1016/j.bbagen.2021.130069

Zendrini, A., Paolini, L., Busatto, S., Radeghieri, A., Romano, M., Wauben, M. H. M., Van Herwijnen, M. J. C., Nejsum, P., Borup, A., Ridolfi, A., Montis, C., & Bergese, P. (2019). Augmented COlorimetric NANoplasmonic (CONAN) method for grading purity and determine concentration of EV microliter volume solutions. *Frontiers in Bioengineering and Biotechnology*, *7*, 452. https://doi.org/10.3389/fbioe.2019.00452

SUPPORTING INFORMATION

Additional supporting information can be found online in the Supporting Information section at the end of this article.

How to cite this article: Radeghieri, A., Alacqua, S., Zendrini, A., Previcini, V., Todaro, F., Martini, G., Ricotta, D., & Bergese, P. (2022). Active antithrombin glycoforms are selectively physiosorbed on plasma extracellular vesicles. *Journal of Extracellular Biology*, *1,* e57. https://doi.org/10.1002/jex2.57